The WSR-88D Rainfall Algorithm

RICHARD A. FULTON, JAY P. BREIDENBACH, DONG-JUN SEO, AND DENNIS A. MILLER

Hydrologic Research Laboratory, Office of Hydrology, NOAA/National Weather Service, Silver Spring, Maryland

TIMOTHY O'BANNON

Applications Branch, WSR-88D Operational Support Facility, Norman, Oklahoma

(Manuscript received 2 May 1997, in final form 18 August 1997)

ABSTRACT

A detailed description of the operational WSR-88D rainfall estimation algorithm is presented. This algorithm, called the Precipitation Processing System, produces radar-derived rainfall products in real time for forecasters in support of the National Weather Service's warning and forecast missions. It transforms reflectivity factor measurements into rainfall accumulations and incorporates rain gauge data to improve the radar estimates. The products are used as guidance to issue flood watches and warnings to the public and as input into numerical hydrologic and atmospheric models. The processing steps to quality control and compute the rainfall estimates are described, and the current deficiencies and future plans for improvement are discussed.

1. Introduction

The Next Generation Weather Radar (NEXRAD) program is a federal triagency program of the National Weather Service (NWS; Department of Commerce), Federal Aviation Administration (Department of Transportation), and Air Force Air Weather Service and Naval Oceanography Command (Department of Defense). It has resulted in the delivery of over 160 S-band Weather Surveillance Radar-1988 Doppler (WSR-88D) radars across the United States (Crum and Alberty 1993; Heiss et al. 1990). The first radars were deployed in 1991 and the last ones in 1997. The NEXRAD program has been a major component of the ongoing technology modernization of the NWS and has revolutionized weather forecasting in the United States. In particular, it has greatly improved the NWS hydrologic forecasting and warning program (Fread et al. 1995; Larson et al. 1995; Stallings and Wenzel 1995).

In addition to standard base data products (reflectivity, Doppler velocity, and spectrum width), the WSR-88D radars use fully automated scientific algorithms to generate value-added hydrometeorological products for use by forecasters (Klazura and Imy 1993). The algorithm that produces rainfall estimates, called the Precipitation Processing System (PPS), is actually a set of ''subalgorithms'' that execute in series. It was designed, developed, and tested over a number of years beginning in the early 1980s at the Hydrologic Research Laboratory under the leadership of M. Hudlow. Today the algorithm remains largely unchanged from its original design. This paper describes the real-time processing steps of the PPS in transforming reflectivity factor measurements into rainfall accumulations for operational forecasting applications, and it updates the original articles describing the initial PPS design (Ahnert et al. 1983; Ahnert et al. 1984; OFC 1991). The result is a comprehensive description of the current state of the PPS as of the latest WSR-88D software release ''Build 9,'' delivered in November 1996. These releases by the WSR-88D Operational Support Facility (OSF) have typically come at roughly one-and-a-half-year intervals and have allowed the WSR-88D-algorithms to mature and evolve over time as operational experience grows.

Details of the fundamentals of radar rainfall estimation and the associated error sources can be found in numerous review articles (e.g., Sauvageot 1994; Joss and Waldvogel 1990; Smith 1990; Austin 1987; Doviak 1983; Wilson and Brandes 1979), though a brief summary relevant specifically to the PPS is presented. There is no attempt made here to discuss how the PPS has performed since the WSR-88Ds were first deployed. The Hydrologic Research Laboratory and its collaborators are performing ongoing performance evaluations (e.g., Seo et al. 1996, 1997; Smith et al. 1996b, Smith et al. 1997), but space limitations prevent including results in this paper. References are appearing in the literature that address those issues (e.g., Smith et al. 1996a,c; Hunter 1996).

Corresponding author address: Richard A. Fulton, Hydrologic Research Laboratory, NOAA/National Weather Service W/OH1, 1325 East–West Highway, Silver Spring, MD 20910.
E-mail: fulton@skipper.nws.noaa.gov

Because reflectivity factor data is the single, fundamental input to the PPS, section 2 describes the data and how it is quality controlled. Section 3 describes each of the major processing steps of the PPS. Rain-gauge data characteristics and communication pathways into the WSR-88D are presented in section 4. Section 5 discusses current deficiencies of the PPS algorithm and plans for future enhancement. Section 6 contains a description of additional rainfall processing that is performed outside of the WSR-88D radar by the NWS River Forecast Centers to improve upon the radar estimates. Finally, section 7 contains concluding remarks.

2. Reflectivity data and quality control

The radar data acquisition (RDA) component of the WSR-88D contains the antenna, tower, transmitter, receiver, and signal processor. During the processing of the returned electromagnetic waves and conversion from analog to digital signals, the equivalent reflectivity factor (hereafter simply called reflectivity) data are computed and calibrated, and clutter signals are suppressed (Heiss et al. 1990; OFC 1992). While these are automated processes, they require some human interaction, and at times the resulting reflectivity data can be biased or contaminated. The PPS attempts to correct for these reflectivity errors, as will be described in section 3.

Chrisman et al. (1994) describes automated procedures to reduce or eliminate nonmeteorological returns from known and persistent ground targets using the Doppler velocity measurements. During clear weather conditions and as often as needed, a clutter map is built using off-line procedures that define the locations of stationary ground clutter. During real-time data collection, suppression is performed for those range bins predefined in the clutter map if their Doppler velocity is near zero. In addition, the radar operator can manually define clutter suppression regions to remove transient anomalous propagation returns if necessary for regions where clutter suppression is not normally performed. These WSR-88D clutter suppression techniques have proven very robust and valuable in reducing cases of rainfall overestimation, but unfortunately, in some rainfall events, rainfall may be underestimated in those limited areas where the rain intersects the zero isodop.

The WSR-88D continuously collects reflectivity, radial velocity, and spectrum-width base data in volume scans composed of 360° sweeps with approximately 1°-wide contiguous sampling in elevation. Volume scans contain data at elevation angles from 0.5° to 20° and have a temporal sampling interval of 5–10 min. Reflectivity data with 0.5-dBZ precision are collected in 1.0-km range bins approximately every 1° in azimuth. This calibrated, quality controlled reflectivity data is currently the only radar data input to the PPS.

3. Algorithm components

The PPS is collectively composed of five main scientific processing components and two external support functions (Fig. 1). The five scientific subalgorithms will be discussed in detail below and are identified as follows: 1) preprocessing (section 3c), 2) rate (section 3d), 3) accumulation (section 3e), 4) adjustment (section 3f), and 5) products (section 3g). The two support functions, precipitation detection (section 3a) and rain gauge data acquisition (section 3b), execute independently of the PPS and provide additional important input information for the main algorithm. Because these two support functions provide input data, they will be discussed first. These subalgorithms of the PPS reside in the radar product generator (RPG) computer along with numerous other meteorological algorithms that process the base data from the RDA to produce value-added products for the forecaster's use.

The PPS algorithm contains 46 adaptable parameters that control how it performs. These parameters can be manually adjusted to allow it to adapt to local meteorological conditions such as rain system type, season, climatology, or other local factors such as topography, radar siting, or rain gauge network characteristics. The requirement to maintain flexibility is critical because this one single algorithm must serve all regions of the United States, from Alaska to Puerto Rico, with greatly varied climatological regimes and topography. As each of the five major subalgorithms and two support functions of the PPS is described in the upcoming sections, the relevant adaptable parameters will be noted. Currently most of the parameters are identical nationwide; however, as greater understanding of the local conditions across the country is gained through operational experience, these parameters are expected to increasingly vary from radar to radar.

a. Precipitation detection

The five major processing steps of the PPS execute in sequence as long as the first support function, the precipitation detection function (PDF; see Fig. 1), determines that rain is occurring anywhere within 230 km of the radar. The PDF has two main tasks to perform every volume scan: to determine the scanning mode of the radar antenna, and to determine the processing mode of the PPS. The PPS can make use of reflectivity data at the lowest four elevation angles, nominally at 0.5°, 1.5°, 2.4°, and 3.4°. If non-ground-clutter reflectivity echoes that exceed predefined intensity and areal coverage thresholds (adaptable parameters called ''significant precipitation'' or ''category one'' thresholds) are present at any of these four lowest elevation sweeps, the PDF will automatically switch the scanning mode of the radar from ''clear air'' to ''precipitation'' mode. This decreases the volume scan interval from 10 min to either 5 or 6 min. The shorter scanning intervals

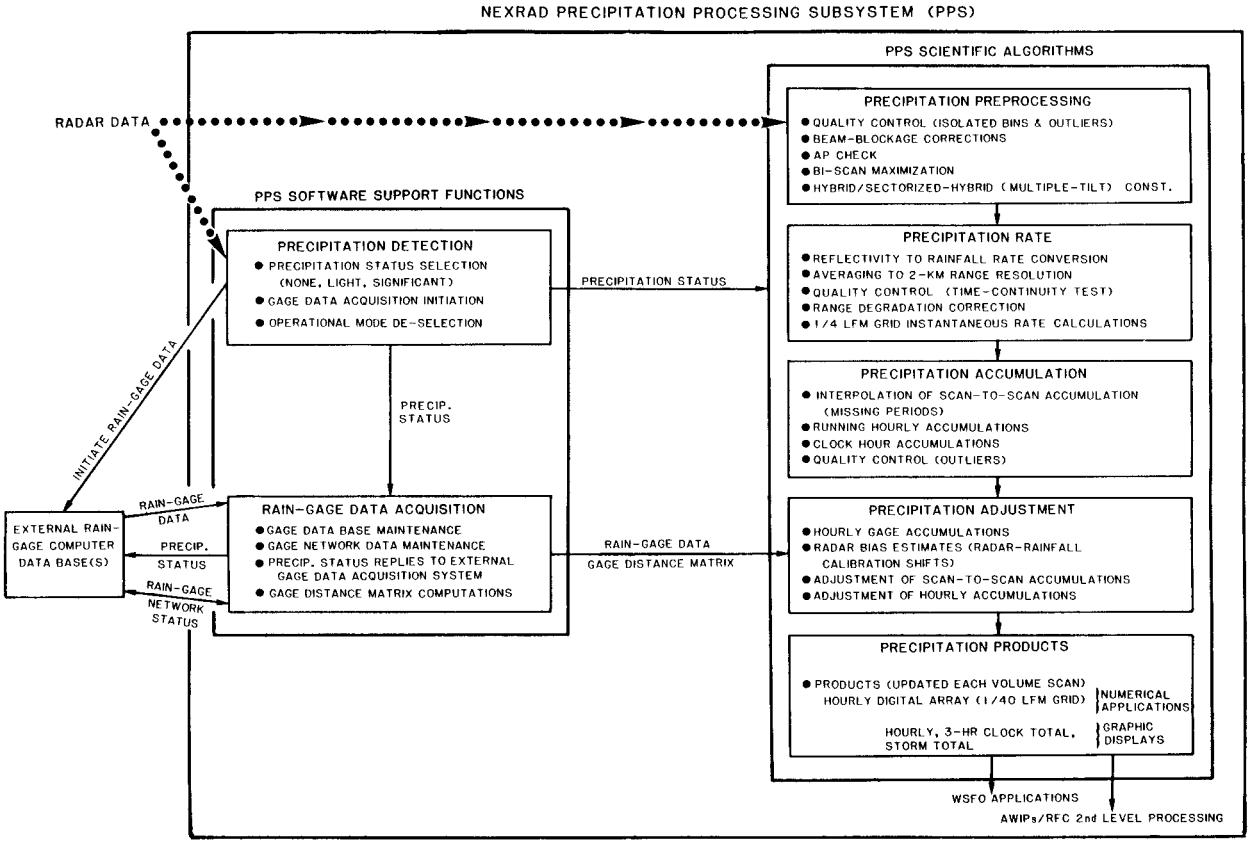

FIG. 1. Schematic overview of the PPS processing sequence for each of the five scientific subalgorithms and two support functions.

associated with the precipitation mode provide more frequent sampling and therefore improved rainfall estimation.

A different set of reflectivity intensity and areal coverage thresholds (called ''light precipitation'' or ''category two'' thresholds) is used by the PDF to determine the processing mode of the PPS, that is, whether it accumulates rainfall or not. This second set of thresholds contains smaller values than the previous category one thresholds, and they correspond to the lowest bounds on resolvable rainfall in the PPS algorithm (i.e., 0.1 mm). If these thresholds are exceeded, the PDF instructs the PPS algorithm to begin accumulating rainfall from an initial zero-valued field regardless of which scanning mode the radar antenna is currently operating in. Under clear air conditions without detectable precipitation (as defined by the PDF category two parameter settings), the PPS operates in a simplified processing mode in order to reduce computer processing. The end of the rainfall event is arbitrarily defined as the end of a 1-h period in which no rainfall is detected by the PDF, and the storm total rainfall product [see section 3g(1)] is then automatically reset to zero initial values.

b. Rain gauge data acquisition

The second PPS support function within the RPG is called the rain gauge data acquisition function (RGDAF). It receives the real-time gauge reports in Standard Hydrometeorological Exchange Format (SHEF) from an external gauge data support (GDS; see Fig. 1 and section 4a) computer and places them into a gauge database within the RPG for use by the PPS. The GDS computer also sends raingauge identifiers and locations to define the network used by each WSR-88D. The RGDAF normally remains dormant until the PDF indicates that rain has been detected within the radar's scanning domain. When this occurs, the RGDAF automatically makes a ''wake-up'' phone call to the external GDS computer and instructs it to start sending real-time gauge reports to the RPG. When the PDF no longer detects rainfall in the radar's domain, the GDS computer receives a message signal from the RGDAF to stop sending gauge data until rain returns.

c. Reflectivity preprocessing

1) CONSTRUCTION OF THE SECTORIZED REFLECTIVITY HYBRID SCAN

Once the precipitation detection function detects rainfall within range of the radar, the first major processing step of the PPS, the preprocessing algorithm, assembles reflectivity measurements from each volume scan into a fixed polar grid with resolution of 1° in azimuth by

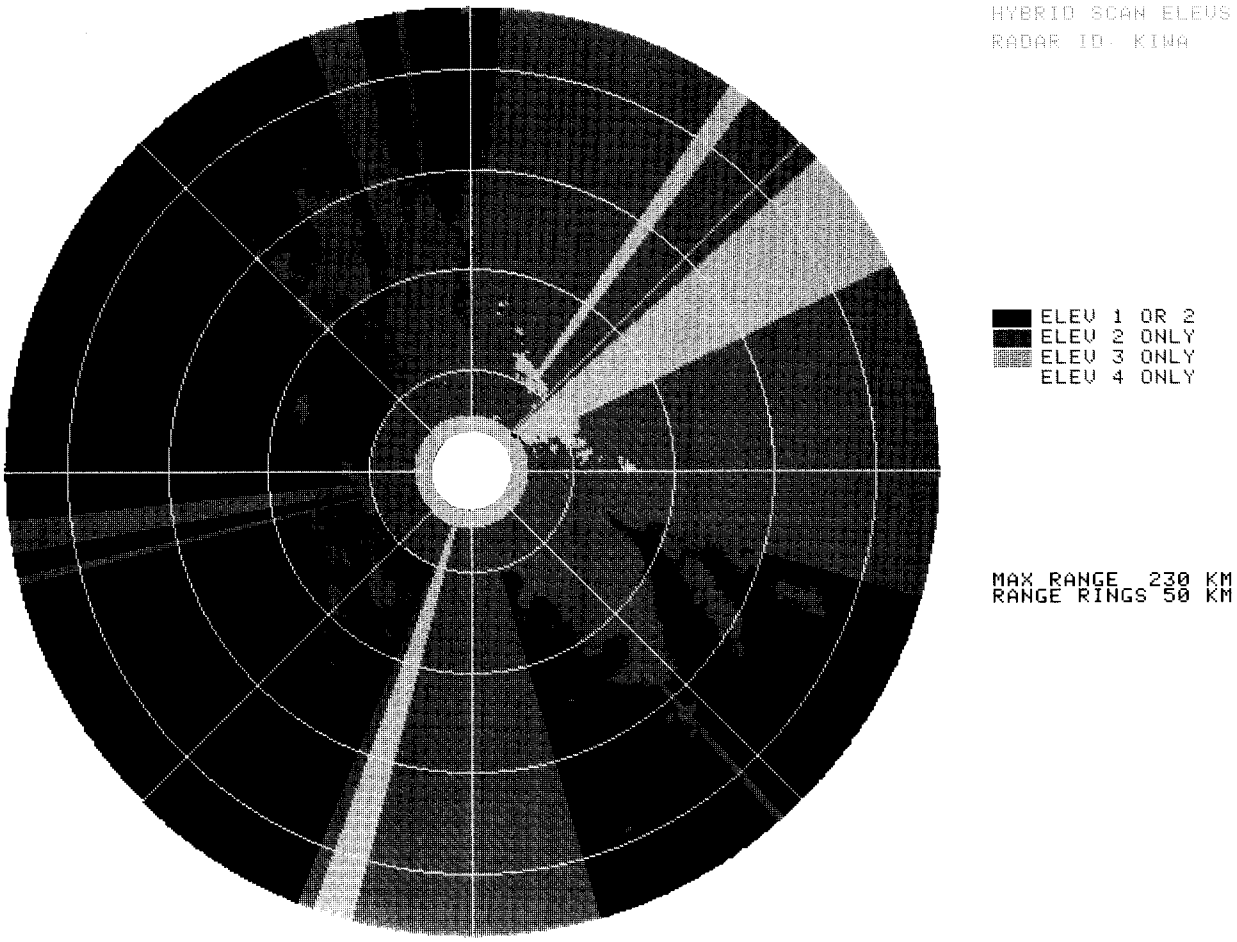

FIG. 2. A graphical depiction of the hybrid scan ''lookup table'' for the Phoenix, AZ, WSR-88D (IWA) showing which elevation angles are used to derive rainfall. The circular tilt angle transitions near the radar occur at 20-, 35-, and 50-km range. Range ring intervals are 50 km, and the maximum range shown is 230 km.

1 km in range out to a maximum range of 230 km. The reflectivity values to be used for each range and azimuth bin are selected from the lowest four elevation angles, or tilts, hence the name ''hybrid scan.'' The azimuths and ranges from which the reflectivity data are extracted to construct this ''sectorized'' hybrid scan depend upon local terrain variations.

The choice of which tilt angle to use for each polar grid point depends on which angle is closest to an ''optimum'' altitude (currently 1.0 km above radar level) unless it is blocked more than 50% by terrain. The bottom of the chosen beam must also clear the ground by at least 150 m. The lowest elevation angle that satisfies these criteria is used. The objective is to utilize reflectivity measurements from as close to 1-km altitude as possible while minimizing the likelihood of ground clutter and data loss due to terrain blockages. The procedure is not as elegant as a true constant-altitude plan position indicator construction using vertical interpolation to a uniform height, but it is computationally efficient.

Each WSR-88D site has a unique, hybrid scan ''lookup table'' in the form of a polar grid at 1 km by one azimuthal degree defining which one of the four lowest elevation angles to use at each polar grid point. This is derived from U.S. Geological Survey three arc-second digital terrain models according to the specified criteria above. It is generated once for each WSR-88D using off-line procedures. The inherent assumptions are that the radar always scans at the predefined elevation angles, and the beam propagates according to standard refraction.

Figure 2 is a graphical depiction of the hybrid scan lookup table for the Phoenix, Arizona (IWA), WSR-88D, which has significant terrain blockage around the radar. Close-in ranges use the fourth tilt, while at longer ranges progressively lower tilt angles are used. However, in the northeast and south sectors, the preprocessing algorithm uses reflectivity data from the second tilt (1.5°) and even the third tilt (2.4°) when constructing the hybrid scan at long ranges. This is due to mountain blockages exceeding 50% at lower angles.

This technique has the advantage of using higher an-

gle data where known terrain features cause significant residual ground clutter or partial or total beam blockage at lower angles. Although data from higher angles does not necessarily represent near-surface conditions, particularly in shallow stratiform rainfall events at far ranges, this simple procedure has shown skill in filling data-void sectors resulting from terrain blockage. More details on the procedure can be found in Shedd et al. (1991).

A new ''terrain-based'' hybrid scan construction procedure is currently being operationally tested at five sites for possible nationwide deployment in the near future. This new procedure is the same as before except the optimum altitude, currently 1.0 km above ground level, is lowered to ground level, which essentially forces the use of the lowest tilt angle that clears the terrain by at least 150 m at each polar grid bin (O'Bannon 1997). It has been shown to effectively mask the tilt transitions in the rainfall products that sometimes cause concentric discontinuities in PPS-derived rainfall near the radar.

2) BISCAN MAXIMIZATION

Biscan maximization (BM) is a procedure in the preprocessing algorithm in which the higher value of reflectivity at either the first (0.5°) or second elevation angles (1.5°) is chosen for a particular polar grid bin during construction of the hybrid scan. This was originally designed as an additional means to minimize underestimation caused by beam blockage at the lowest elevation angle. However, case studies and long-term statistical analyses have shown that BM can inadvertently introduce and enhance undesirable range-dependent overestimation biases in the range interval of approximately 50–150 km due to the intersection of the second tilt angle with the bright band (Seo et al. 1995; Smith et al. 1996b, 1997). Initially, BM was executed over all ranges of the radar; however, because of the above problem, an adaptable parameter was changed in February 1996 so that it is now performed only at ranges beyond 180 km, which is the approximate mean range where the second elevation angle is above the bright band in midlatitudes. Although currently brightband contamination of the rainfall estimates cannot be avoided when tilt angle one intersects it, this change has removed overestimation where the second tilt angle does.

3) PARTIAL BEAM BLOCKAGE CORRECTION

In addition to the hybrid scan lookup table, there is another location-dependent table defining the amount of two-way beam intensity blockage, or occultation, due to terrain features. It is defined for each of the four lowest tilt angles as a function of range and azimuth. The occultation data are used to correct reflectivity measurements along each radial at each of the four lowest angles according to the beam obscuration percentages defined in Table 1. No correction is made for bins in which the blockage of the beam exceeds 60% because if that occurs the next higher tilt angle is used when constructing the hybrid scan.

TABLE 1. Partial occultation corrections.

Occultation (%)	Reflectivity correction (dBZ)
0–10, >60	0
11–29	+1
30–43	+2
44–55	+3
56–60	+4

4) CORRECTION FOR ISOLATED TARGETS AND GROUND CLUTTER

This quality control step removes reflectivity data that are abnormally large in magnitude but small in area, such as those associated with nonmeteorological targets (airplanes, anomalous propagation returns, or residual ground clutter). Two reflectivity thresholds are used here. Isolated sample bins are defined as polar bins with reflectivities that exceed a certain threshold (an adaptable parameter currently set at 18 dBZ) and for which no more than one of the eight surrounding neighbors is also above that same threshold. Isolated bins are replaced with a reflectivity of 0 dBZ.

A second maximum reflectivity threshold parameter (currently set at 65 dBZ) is used to quality control the extremely large point outlier reflectivity bins typically associated with residual ground clutter or anomalous propagation that have not previously been removed by clutter suppression at the RDA. If a grid bin has a reflectivity that exceeds this threshold, it is replaced with either an average of surrounding values if none of them are above the same threshold, or otherwise it is assigned a very small value (7 dBZ; an adaptable parameter). This step will not remove all occurrences of residual clutter or anomalous propagation, and hence additional quality control steps are necessary.

5) TILT TEST AND ANOMALOUS PROPAGATION

Strong vertical temperature and moisture gradients in the lower atmosphere can cause the beam to superrefract and produce echoes from ground targets that may be misinterpreted as rainfall. Earlier clutter suppression procedures in the RDA can remove most of these echoes; however, additional quality control procedures are necessary within the PPS. The ''tilt test'' is another automated quality control procedure designed to remove the deleterious overestimation caused by anomalous propagation (AP). The tilt test is a vertical echo continuity check that uses knowledge that the areal extent of AP often rapidly decreases as the antenna elevation steps up to higher angles. When the algorithm detects

a decrease in the total reflectivity echo area exceeding 75% (an adaptable parameter) from the first to the second elevation angles over the annular area between the range of 40 to 150 km (adaptable parameters), the algorithm discards all the reflectivity data from the lowest tilt angle and uses only the data from the second or higher tilts in the construction of the hybrid scan for that particular volume scan.

This vertical continuity procedure is primitive, yet it has proven operationally effective for removing most AP in situations where real rainfall does not exist within range of the radar. It is in the more challenging situations when rain and AP coexist that the tilt test is more likely to fail. Effective use of transient ground clutter suppression procedures at the RDA can significantly reduce the amount of AP contamination in these situations (Chrisman et al. 1994). Additional automated and human-interactive quality control procedures currently exist outside of the WSR-88D in follow-on radar rainfall processing performed in stages II and III at the NWS River Forecast Centers (see section 6).

d. Rain-rate conversion

1) Conversion from reflectivity to rain rate

The rate algorithm is the second main processing step of the PPS. It executes every volume scan following the completion of the preprocessing algorithm. It converts reflectivity factor data from the hybrid scan into rain rates using a standard *Z–R* power law relationship derived from the empirical relationship between the two variables (e.g., Battan 1973; Doviak and Zrnić 1984). The current default equation is

$$Z = 300R^{1.4},$$

where Z has units of mm^6 m^{-3} and R in mm h^{-1}. Some sites located in more tropical environments use an alternate relationship,

$$Z = 250R^{1.2},$$

which is generally better for tropical rainfall events (Rosenfeld et al. 1993). The algorithm retains precision to the nearest 0.1 mm h^{-1} during the log-to-linear conversion.

Once the rain rates are computed on the 1 km $\times$ 1° grid, averaging is performed on adjacent pairs of radial bins. The result is a polar grid of rain rates, called the rate scan, with spatial resolution of one azimuthal degree by 2 km in range. This fixed polar grid is the basis for all subsequent processing in the PPS and represents the smallest spatial scale for rainfall estimates from the WSR-88D. With the fixed 1° azimuth grid of the PPS, the scale of rainfall estimates range from 2 km (in range) $\times$ 4 km (in azimuth) at the maximum range of radar rainfall estimates (230 km), to 2 km $\times$ 2 km at midranges (115 km), to 2 km $\times$ 0.3 km at close ranges (20 km).

The *Z–R* parameter settings are designed to be adjustable at each site; however, a challenge exists in formulating and providing proper guidance to the forecasters on what particular *Z–R* parameters are most appropriate for a given rainfall event before the rainfall begins. No such objective, definitive guidance is currently available.

2) Correction for hail

Because the *Z–R* power law produces unreasonably large instantaneous rain rates in the hail cores of thunderstorms, it is necessary to cap them at a maximum value expected to be associated with rain only. The ''hail cap'' threshold, an adaptable parameter representing the maximum expected instantaneous, rain rate, has typical values ranging from about 75 mm h^{-1} (3 in. h^{-1}) to about 150 mm h^{-1} (6 in. h^{-1}) except in highly unusual events. Using the standard NEXRAD *Z–R* relationship, these values translate to about 51 and 55 d*BZ*, respectively. The nationwide default setting of the hail cap is currently 104 mm h^{-1} (53 dB*Z*), but a number of radar sites in more tropical environments along the gulf coast use higher values such as 150 mm h^{-1}. Likewise, some sites in the dry mountainous west use the lower value of 75 mm h^{-1}.

The choice of which hail threshold to use can significantly impact the resulting rainfall estimates depending on the areal extent of the hail cores and the speed of the storms. Unfortunately it is very difficult to objectively determine the appropriate setting for a particular day or storm. There have been some studies relating the hail threshold to various ambient atmospheric sounding parameters such as precipitable water or surface dewpoints (Kelsch 1992). Until more studies are performed, or until additional microphysically based radar polarization information becomes available, we are necessarily left with somewhat arbitrary hail thresholds to prevent overestimation from hail.

3) Time continuity test

A quality control step is performed in the rate algorithm that compares the change in volumetric rain rate over the radar scanning domain with that computed in the previous volume scan. If there is an increase or decrease beyond a certain reasonable threshold (an adaptable parameter) expected from normal precipitation development or decay, the entire rate scan for that volume scan is discarded. Such a large change could result from spurious radio frequency interference, transient system noise, or AP.

4) Range degradation correction

The capability exists to correct the rain rates to account for signal degradation from partial beam filling, which may reduce the estimates at far ranges. The equa-

tion depends on both range, r (km), and rain rate, R (mm h^{-1}), as follows:

$$R_{\text{corr}} = aR^b r^c,$$

where a, b, and c are coefficients to be derived from local studies. Until enough long-term data are collected from many sites to confidently estimate the coefficients, they remain at the values 1, 1, and 0, respectively, for all sites, implying no range correction.

Two range degradation problems that are more significant compared to beam filling are rainfall underestimation due to overshooting the rain at far ranges (a problem of lack of detection) and vertical gradients of reflectivity. These effects are not currently accounted for in the PPS.

e. Rainfall accumulation

1) INTEGRATING RATE SCANS

The accumulation algorithm performs a simple integration of consecutive rate scans over the 5-, 6-, or 10-min period spanning two volume scans. A linear average rain rate is computed at each 2 km $\times$ 1° polar grid bin from the two consecutive rate scans, and that rate is applied over the scan-to-scan period. Each of these scan-to-scan accumulations is then summed over time from the beginning of the rain event to produce a storm total rainfall accumulation. The internal precision of the accumulations on a linear scale is retained at 0.1 mm.

2) ACCOUNTING FOR MISSING PERIODS

There is a possibility that consecutive rate scans could span a much longer time period than the usual 5-, 6-, or 10-min period because of radar hardware or software problems. Because the error associated with the accumulation grows as the time between consecutive rate scans increases, a limit, currently 30 min, is imposed on the amount of time over which the linear interpolation of rain rates is performed. If a gap larger than 30 min exists, the excess period midway between the two scans is assumed to contain missing data. There is a procedure to fill in the two 15-min periods immediately after the last good rate scan and immediately before the next good rate scan by extrapolating a 15-min accumulation from those single rate scans assuming that the rain rates are constant. If the time between scans exceeds 36 min (based on two adaptable parameters), no scan-to-scan and hourly accumulation products are generated.

3) REMOVAL OF HOURLY OUTLIERS

A final step in the accumulation algorithm removes bins in which the hourly accumulation exceeds a maximum threshold. If any hourly accumulation bin exceeds the outlier threshold (currently 400 mm) and its eight neighbors are below the threshold, that outlier bin is replaced with the average of its neighbors. If all eight neighbors are not below the threshold, a different maximum threshold is used to cap the hourly radar accumulations.

f. Gauge–radar adjustment

Real-time rain gauge data can be used to adjust the radar rainfall estimates in the fourth PPS algorithm, adjustment. Currently, this algorithm is not being executed operationally because the necessary communication system between the gauges and the WSR-88D has not yet been completed (see section 4a).

A temporally fixed Z–R relationship, as is the current design of the PPS, will not be appropriate for all rainfall events. Because it is not currently feasible to manually adjust the Z–R parameters in real time due to the lack of proven, robust, and objective criteria valid over a broad range of rainfall types, it is useful to make automated adjustments to the rainfall estimates by comparing them with real-time rain gauge data on an hourly time step. The net effect of this hourly adjustment procedure is an automated, objective tuning of the multiplicative coefficient in the Z–R relationship (e.g., the 300 in the equation $Z = 300R^{1.4}$). This adjustment, in the form of a gauge–radar (G–R) multiplicative bias, is performed uniformly over each WSR-88D scanning domain, and therefore it is called the ''mean field'' bias adjustment. This multiplicative factor is applied to the scan-to-scan incremental radar estimates. A value of 1.0 implies no bias, a bias of greater than unity implies a radar underestimate, and a value between 0.0 and 1.0 implies a radar overestimate relative to the gauges.

Because these computed hourly biases are representative of the total area over which gauge and radar data are available, they do not account for spatial variability of bias within individual storms nor any range or azimuth-dependent biases that may exist. Also, because the bias estimation algorithm uses a statistically based Kalman filter formulation, the larger the sample of hourly gauge data available, the more representative the resulting gauge–radar bias estimate will be. The computed bias is expected to account for spatially uniform radar estimation errors such as hardware miscalibration, wet radome attenuation, and inappropriate Z–R coefficients.

1) ASSEMBLY OF HOURLY GAUGE ACCUMULATIONS

The adjustment algorithm computes gauge–radar biases using pairs of collocated hourly gauge and radar accumulations. The first step is the assembly of hourly gauge accumulations. As will be discussed in section 4, the external gauge data support computer will provide real-time gauge data to the RPG for a predefined set of gauges (currently up to 50). That list of gauges is ordered in sequence by examining the distance of each gauge from all the others. This distance information is

used to order the gauges so that the gauges at the top of the list are the most widely spaced relative to their neighbors and therefore are likely to provide the most spatially independent rainfall information. This ordering is important because only the top 30 raingauges that report rain for a given hour are chosen from the list to be used in the algorithm. These gauge limits will be increased in the near future. The adjustment algorithm has been designed to make use of both incremental and accumulator gauge measurements at whatever temporal reporting frequency they are available.

Currently the hourly period of gauge–radar comparison is from the top of one hour to the top of the next (H + 00 min; an adaptable parameter). This parameter setting has been optimized to reflect the predominant reporting characteristics of existing gauge networks available to the NWS (see section 4b). It is necessary to take the available accumulator gauge measurements and interpolate them to values at the top of each hour if such information is not directly available. The associated error in the interpolation grows with the interpolation period, so there is a limit placed on the time period over which an interpolation is done (15 min; an adaptable parameter). No hourly gauge accumulation is considered usable for an accumulator gauge if there are no reports within 15 min of both the beginning and end of the hourly period. Clearly any gauge with reports valid exactly on the top of the hour will require no interpolation, and fortunately we have found that the largest number of operationally available accumulator gauges report at this time.

Likewise, incremental accumulation reports that are not 1-h duration and do not end at H + 00 also need to be distributed into the desired 1-h period by partitioning the existing incremental reports and assuming constant rain rate over the period.

2) Assembly of hourly radar accumulations

Associated with each available 1-h gauge accumulation is the corresponding radar accumulation. The accumulation algorithm provides hourly polar accumulation arrays from the radar ending exactly at the top of the hour. The adjustment algorithm extracts from this hourly radar accumulation scan the nine polar bins closest to each raingauge. If the range of radar accumulations in these nine bins spans the gauge accumulation value, then an exact match gauge–radar pair is created for that gauge. If the nine radar values do not span the gauge value, the closest radar accumulation to the gauge value from the nine bins is chosen to form the gauge–radar pair.

There are a number of reasons why the surrounding nine bins are examined. First, there may be errors associated with the imprecise knowledge of the locations of the raingauges (see section 4b). Many gauges have latitude and longitude locations precise only to the nearest minute (approximately 2 km in midlatitudes), which is approximately the spatial resolution of the radar rainfall estimates at middle ranges. Second, there may be errors in calibration of the WSR-88D antenna azimuth angles on the order of a degree or so, which is the azimuthal resolution of the PPS estimates. Third, horizontal displacement of the radar-measured rainfall aloft and the gauge at the ground can lead to errors.

3) Quality control of gauge–radar pairs

In addition to the more obvious and well-known error sources associated with radar rainfall estimation and the sampling size differences associated with comparing point gauge and volume-averaged radar data, there are numerous other error sources that are often hard to quantify. These may include 1) mismatch of radar and gauge clocks, 2) errors associated with temporal interpolation of gauge reports assuming linear rain rates, 3) gauge undercatch associated with intermittent power outages during electrical storms or extreme rain rates (tipping bucket gauges only) and wind effects around the gauge orifice, 4) bad gauge reports due to hardware malfunctions or communication problems, 5) fundamental problems in gauge and radar measurement in snow and mixed precipitation events (including bright band), 6) errors in gauge latitude–longitude locations, and 7) improperly calibrated radar antenna pointing angle (the last two of which may lead to spatial mismatches of gauge and radar observations as previously mentioned). Most of these are gauge-related deficiencies that certainly bring into question the validity of the term ''ground truth,'' often used interchangeably with raingauge data when comparing with radar data. Therein lies the fundamental difficulty in trying to align the two independent measurements of rainfall from radar and raingauge, each of which has its own unique deficiencies.

Because of the variety of errors associated with both gauge and radar data, it is necessary to quality control the gauge–radar pairs every hour before passing them on for further processing. The first quality control step in the adjustment algorithm is the exclusion of any ''nonraining'' pairs, that is, any pairs in which either the hourly gauge or radar rainfall is below a minimum threshold (currently 0.6 mm; an adaptable parameter). This would remove any pairs in which, for example, the gauge is receiving rain but is not recording accurately due to hardware problems, or when the radar sees virga but the gauge is not receiving rain at ground level. Also, the pair would also be excluded from further bias computational processing if the radar is overshooting the rain clouds at long ranges while the gauge is recording rainfall properly.

The second step is to discard any pairs in which the 1-h gauge accumulation exceeds a maximum threshold of 400 mm (an adaptable parameter). The third step is to discard any remaining pairs in which the normalized absolute difference between the hourly gauge and radar rainfall exceeds a maximum threshold number of stan-

dard deviations from the mean difference. The threshold is an adaptable parameter currently set at 2.0 standard deviations. In other words, this test excludes any gauge–radar pairs whose rainfall difference falls outside of two standard deviations for all pairs for that hour, thereby removing any outlier pairs falling in the tails of the distribution. There are several situations where this is important. An example is for a gauge lying at the range where the radar intersects the bright band, in which case the radar may be significantly overestimating the rainfall compared to the gauge below.

4) KALMAN FILTER BIAS ESTIMATION

The collocated gauge–radar pairs are assembled for 1-h periods ending at the top of the hour. However, because it takes time to transmit the data from the gauge platform to the data collection system and ultimately to the RPG, there must be a built-in time delay in the actual assembly and use of the gauge–radar pairs within the PPS adjustment algorithm after the gauges collect their measurements. Currently the delay can be no more than about 50 min (an adaptable parameter), that is, the 1-h gauge and radar data for the 1-h period ending at 1300 UTC, for example, are not assembled until about 1350 UTC, giving time for the real-time gauge data for that period to be received by the RPG. At this time each hour the adjustment algorithm performs quality control of the gauge–radar pairs, and a new bias is computed if a minimum threshold number of gauge–radar pairs is generated (currently six; an adaptable parameter). That new bias is then applied to the current and future scan-to-scan radar estimates until a new bias is computed the next hour. Thus there is an unavoidable 2-h or so maximum delay introduced by delays in communication paths of the gauge data and the 1-h accumulation period. If the true mean-field bias changes at shorter timescales than an hour or two, the adjusted PPS rainfall estimates will not adequately reflect these fast time-varying changes.

Once a set of quality controlled gauge–radar pairs is assembled (currently at least 6 and at most 30 pairs), the adjustment algorithm makes an estimate of the true, unknown bias through an implementation of a discrete Kalman filter (Gelb 1974; Ahnert et al. 1986) to determine the statistical significance of the paired observations as estimators of the true unknown bias. Gauge and radar sensor errors as well as sampling errors are incorporated into the formulation through the statistics (scatter) of the gauge–radar observations. The Kalman filter optimally weighs the new sample pair observations each hour with those from previous hours to determine how informative the most recent pairs are. Statistical measures of the information content of the latest observation pairs, in terms of mean error variance of the gauge and radar estimates compared with similar measures contained in a mathematical bias model, determine the extent to which the new pairs will impact and adjust the bias estimated from the preceeding hours. The mathematical bias model presumes that the bias follows a random walk process; that is, the bias is equally likely to increase or decrease from one hour to the next. Based on this model, the best model forecast for the next hour is simply the best current estimate for the current hour.

Wide scatter in scatterplots of the gauge–radar pairs (large mean square error) implies a relatively small informativeness of the current observed data; tight scatter implies a relatively large informativeness. In the former case, the model-predicted bias from the previous hour is most heavily weighted compared to the sample G/R bias, B_{sample}, from the current hour where,

$$B_{\text{sample}} = \sum G_i / \sum R_i,$$

where $i = 1$, number of pairs for current hour. In the latter case, the current sample bias is more heavily weighted than the model-predicted bias. Two adjustment algorithm adaptable parameters affect how compliant the Kalman filter bias estimates are to the sample observations each hour, that is, how much filtering of the sample G/R ratios is performed.

If forecasters determine that the computed bias estimate for any particular hour is not reasonable, they can choose to not apply it to the rainfall estimates through the use of a manually controlled on/off toggle parameter. In any event, the adjustment algorithm continues to execute automatically in the background once an hour. If an insufficient number of pairs is available to compute a bias for a given hour (due perhaps to the end of the rain event), the bias estimate from the previous hour is propagated forward for 1 h. If the situation continues, the most recently computed bias estimate linearly drifts back to a reset bias value (an adaptable parameter currently set at 1.0) over a fixed number of hours (another adaptable parameter currently set at 12 h).

Because of the ability of the Kalman filter to make use of the statistics of the observations to optimize the bias estimates, this technique is expected to provide more reliable bias estimates than those calculated from simple mean hourly G–R ratios (e.g., as described in Klazura and Kelly 1995). More detailed information on the mathematics of the Kalman filter as applied to the gauge–radar bias estimation procedure in the PPS can be found in Ahnert et al. (1986). Smith and Krajewski (1991) describe a similar procedure.

The Hydrologic Research Laboratory is actively examining an alternative and improved formulation for gauge–radar adjustment that utilizes gauge and radar accumulations over longer time periods than the current 1 h (Seo et al. 1997), and likely this subalgorithm will change significantly in the near future.

g. Rainfall product generation

The last processing step of the PPS is the products algorithm. It is here where rainfall accumulation arrays are formatted into products of varying temporal, spatial,

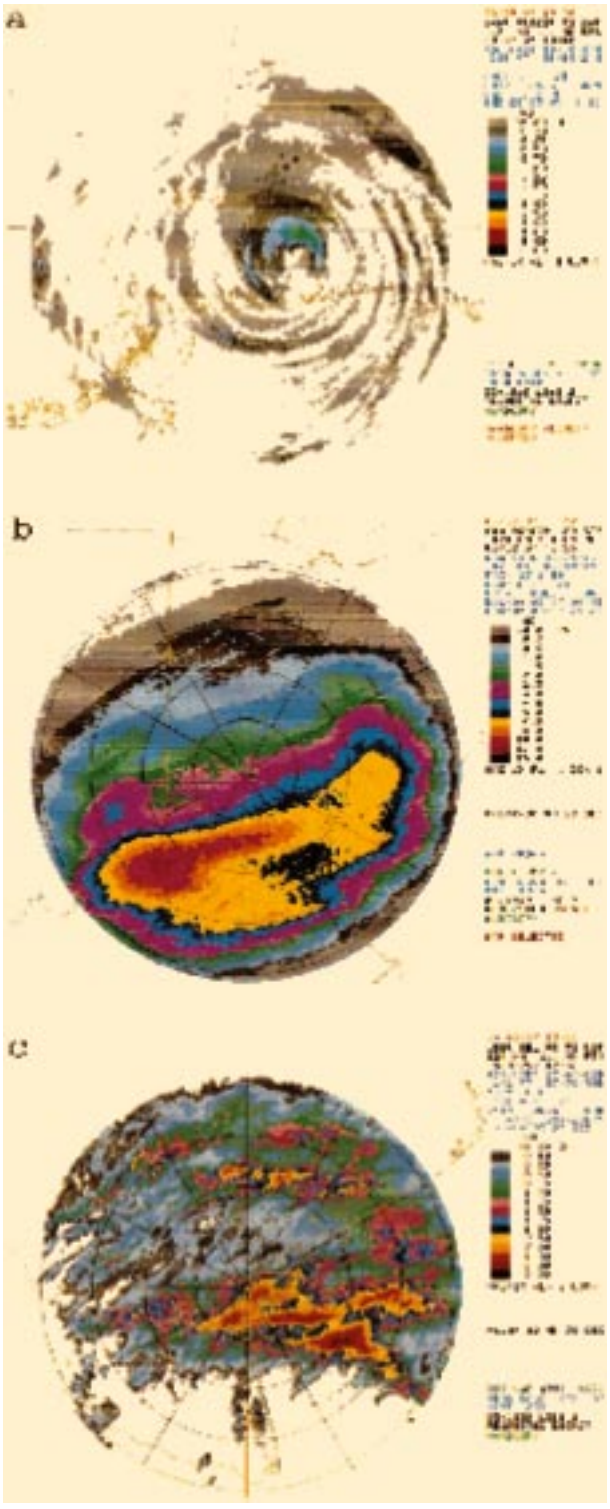

FIG. 3. (a) A 1-h rainfall product (OHP) ending at 1912 UTC 3 August 1995 from the Mobile, AL, WSR-88D (KMOB) associated with the landfall of Hurricane Erin. The maximum accumulation is 1.2 in. near the eyewall, and the maximum range at the edge is 230 km. (b) A storm total rainfall product (STP) from the Wilmington, OH, WSR-88D radar (KILN) for the period 0031 UTC 1 March–1929 UTC 2 March 1997. The maximum estimated rainfall is 13.6 in. to the southwest of the radar. The range rings are at 56–km (30 n mi) intervals. Range degradation of the rainfall estimates is evident (see section 5c). (c) A user-selectable rainfall product (USP) of 24-h duration ending at 1200 UTC 3 April 1997 from the Corpus Christi, TX, WSR-88D radar (KCRP).

and data resolution scales every volume scan for various operational forecasting uses. The RPG then sends these formatted products to the principal user processor (PUP), an external interactive color workstation, to be displayed, manipulated, looped, zoomed, etc. These products are also sent to users outside of the NWS through the NEXRAD Information Dissemination Service (Klazura and Imy 1993). There are currently four graphics products, two digital products, and one alphanumeric product produced by the PPS.

1) GRAPHICS PRODUCTS

The four graphics rainfall products available to the forecaster at the PUP include (a) a 1-h running total; (b) a 3-h total; (c) a storm total; and (d) a user-selectable period accumulation product. All graphics products have been quantized and degraded to 16 data levels from the internal PPS precision of 0.1 mm in order to be displayed on the PUP. The 16 data levels can be adjusted for each product by the forecasters. The products are displayed on the $1^\circ \times 2$ km polar grid just as they have been processed in the PPS algorithm. Various geopolitical maps such as state and county borders and streams can be overlaid.

The 1-h rainfall product is a running accumulation valid from the current volume scan back one hour. It is updated as the PPS executes each new volume scan. Figure 3a is an example of such a product. Various descriptive information is printed on the right side, such as the radar name, current time, and maximum accumulation. The 3-h rainfall product is a 3-h accumulation ending at the most recent clock hour, that is, H + 00 min. It is updated only once per hour at the top of the hour. The storm total rainfall product (Fig. 3b) is a product reflecting rain that has accumulated since the most recent 1-h rain-free period and is updated every volume scan. The user-selectable rainfall product allows the forecaster to choose whatever time period of accumulation is desired. Accumulation periods as long as 24 h are available for display, selectable from the most recent 30 h. Figure 3c is an example of a 24-h rainfall product ending at 1200 UTC.

Each graphic product has a separate alphanumeric product paired with it that contains information such as the setting of the associated PPS adaptable parameters and other supplementary information from the PPS algorithm including the gauge–radar bias estimate and its error variance.

2) ALPHANUMERIC SUPPLEMENTAL PRODUCT

The supplemental precipitation data product is viewed at the PUP's alphanumeric terminal and contains three sections of information. First is a listing of selected supplemental data generated by the PPS algorithm including the current bias estimate, its error variance, whether the bias is being applied to the products, the number of isolated bins and outliers, the reduction in echo area as computed in the tilt test, and the times of any missing periods. The second section contains a listing of all available gauge–radar pairs from the most recent hour, their locations, and whether each pair passed the quality control steps. The third section contains the recent raw gauge reports exactly as they were received by the WSR-88D.

3) DIGITAL PRODUCTS

There are two additional digital products that are generated by the PPS. ''Digital'' implies products that retain the raw data precision in the algorithm, that is, no quantization to broader data levels as done in the graphics products. By retaining the original data resolution, these products can be used in quantitative processing algorithms outside of the WSR-88D system.

The first digital rainfall product is the hourly digital precipitation array (abbreviated either DPA or HDP). This product is generated and updated every volume scan and is a running 1-h rainfall accumulation. The rainfall data are converted from linear internal units of rainfall to a logarithmic scale of 256 data levels with precision of 0.125 dB*A* $\langle 10 \log[\text{accumulation} \times (1\ \text{mm}^{-1})]\rangle$ in order to fit efficiently into a one-byte computer word. The data ranges from -6 dB*A* (0.25 mm or 0.01 in.) to 26 dB*A* (about 400 mm or 15 in.). The rainfall array is run-length encoded to reduce storage and transmission costs and contains various other supplemental information in header and trailer sections. Figure 7a (section 6a) is a graphical representation of a DPA product.

The spatial resolution of this product differs somewhat from the internal polar arrays in which the accumulations are computed. The polar array of hourly rainfall is remapped onto a polar stereographic projection called the Hydrologic Rainfall Analysis Project (HRAP) grid, which is a higher-resolution, nested grid within the familiar Limited Fine Mesh grid used previously in NWS atmospheric numerical models (Schaake 1989). This HRAP grid covers the conterminous 48 states, and the DPA product is mapped to this common grid so that it can be mosaicked with other DPAs across the country in subsequent regional and national rainfall processing (sections 6b and 6c). The grid size is nominally 4 km on a side, ranging from about 3.7 km at southern U.S. latitudes to about 4.4 km at northern U.S. latitudes. A square grid of 131 $\times$ 131 points, centered at the radar, covers the 230-km range domain of the WSR-88D rainfall estimates.

The second digital product from the PPS is actually not a rainfall product. The digital hybrid scan reflectivity (DHR) product is a processed reflectivity product that is output from the first PPS algorithm, the preprocessing algorithm. It contains processed reflectivity data from the hybrid scan on a $1^\circ \times 1$ km polar grid with a precision of 0.5 dB*Z* over the data range -32 to 95 dB*Z*. It is used in off-line flash flood warning applications.

4. Rain gauge data collection and processing

Section 3f described how the PPS adjusts the rainfall estimates using real-time rain gauge data. This section describes the characteristics of the gauge data and how it is passed to the radar.

a. Gauge data support

The NWS Office of Hydrology is currently developing and testing a gauge data support (GDS) capability to provide real-time rain gauge data to each WSR-88D for use in the PPS adjustment algorithm. GDS embodies both hardware and software to provide a data collection, management, and communication system external to the WSR-88D. It automatically collects data from diverse gauge networks into a single local database for all gauges that are operationally available within the 230-km range domain of each radar. It communicates with the WSR-88D through modems and commercial phone lines on an hourly basis when rain is occurring.

The GDS capability is in the final testing phase. Initially the plan is to deploy interim GDS systems as special-purpose hardware systems at three river forecast centers (RFCs) only. Each of these interim GDS systems will support multiple WSR-88D radars located within those RFC's forecast areas. Once the Advanced Weather Interactive Processing System is deployed nationwide, it will host the GDS capability at each of the weather forecast offices collocated with a WSR-88D, eventually replacing the interim RFC-based GDS systems.

b. Gauge networks and characteristics

The NWS makes use of existing automatic telemetering gauge networks that can be interfaced with existing NWS data communication systems in order to support WSR-88D rainfall processing. Special-purpose raingauge networks have not been installed by the NEXRAD program. In fact, a large majority of telemetering gauges used operationally by the NWS are actually owned and operated by other federal, state, and local agencies, primarily the Army Corps of Engineers, Federal Aviation Administration, Department of Agriculture, Natural Resources Conservation Service, and the U.S. Geological Survey. These gauges are accessed by the NWS through interagency data sharing agreements.

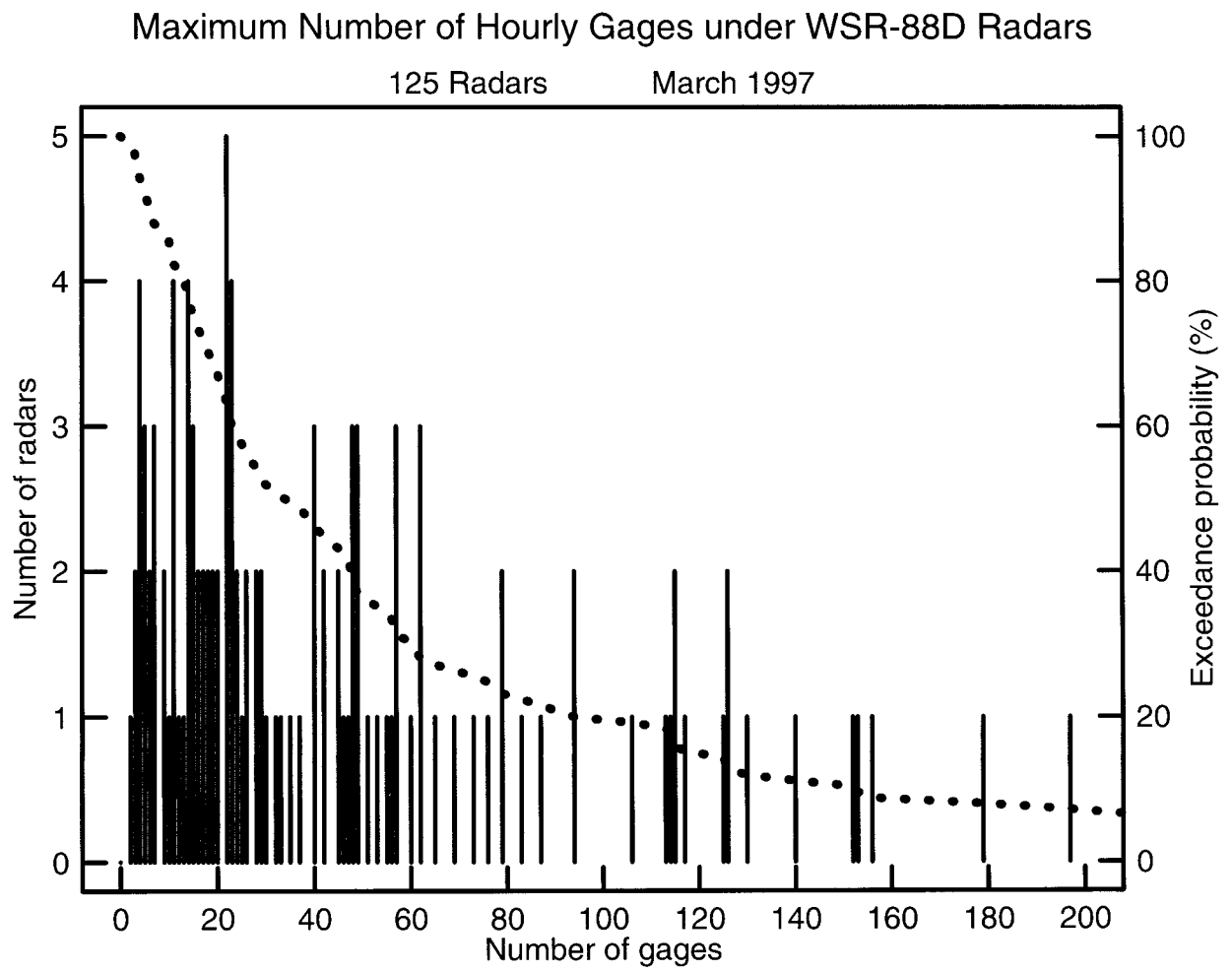

FIG. 4. Histogram of the maximum number of automated, hourly reporting rain gauges per radar within the 230-km scanning domain of a sample of 125 WSR-88Ds, excluding radars in the southwestern United States, Alaska, and Hawaii, as polled during March 1997. The dotted line shows the probability that a radar has greater than a certain number of rain gauges (right-hand axis labels).

The gauge networks that support the NWS hydrology program include the Automated Surface Observing System, (ASOS), Automated Local Evaluation in Real Time, (ALERT), Integrated Flood Observing and Warning System, (IFLOWS), GOES DCP (Geostationary Operational Environmental Satellite Data Collection Platform), and NWS-owned Limited Automatic Remote Data Collectors (LARC). These networks will all supply gauge data to the WSR-88D via the GDS computer along with other regional or local mesonets if available. They include tipping bucket and weighing gauges. They have varying data precision, siting integrity, reporting frequencies, and data quality depending on the agency that owns them, and the NWS has limited control over this.

The vertical bars in Fig. 4 show the maximum number of automated gauges within 230 km of WSR-88Ds that reported for any hour during a 1-month period. These data from a sample of 125 radars were collected during March 1997 from the operational gauge databases at 10 of the NWS river forecast centers (RFCs) where such information was readily available. The dotted line indicates the probability that a given radar has greater than a certain number of gauges within its 230-km range domain. Fifty percent of the radars have at least 34 gauges; 25% (75%) have at least 75 (15) gauges. These numbers likely represent a somewhat conservative estimate of the total number of gauges that may be available in the future for use in the PPS as many of the RFCs are increasing the real-time gauge data flow into their computer databases.

One of the most important requirements of rain gauges for operational use is quick access to the data once it is collected by the gauge. Figure 5 shows the delay between the time of the automated rain gauge measurement and the time the report is actually received and posted into the gauge databases at the RFCs for all telemetering gauges within 230 km of the WSR-88Ds at Charleston, West Virginia (RLX; Fig. 5a), and Tulsa, Oklahoma (INX; Fig. 5b). Two arbitrary 48-h periods

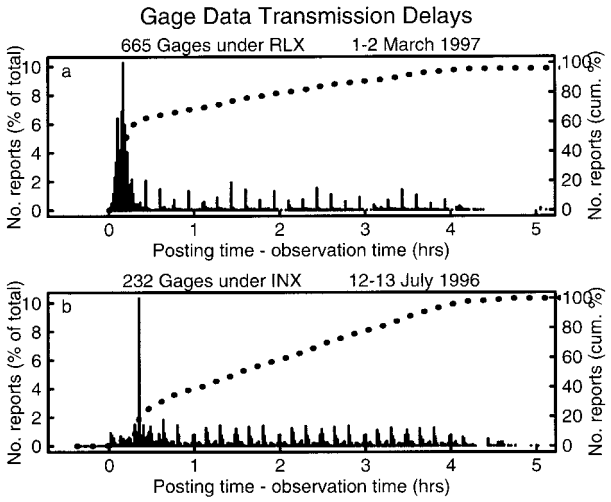

FIG. 5. Time difference between when the rain gauge measurements are collected and posted into the RFC database for all telemetering gauges within 230-km range of the (a) Charleston, WV, WSR-88D (RLX) and the (b) Tulsa, OK, WSR-88D (INX) for two arbitrary 48-h periods. The vertical bars represent the probability density function of the number of gauge reports as a function of time delay (left-hand axis labels), and the dotted line represents the cumulative density function of the number of gauge reports (right-hand axis labels).

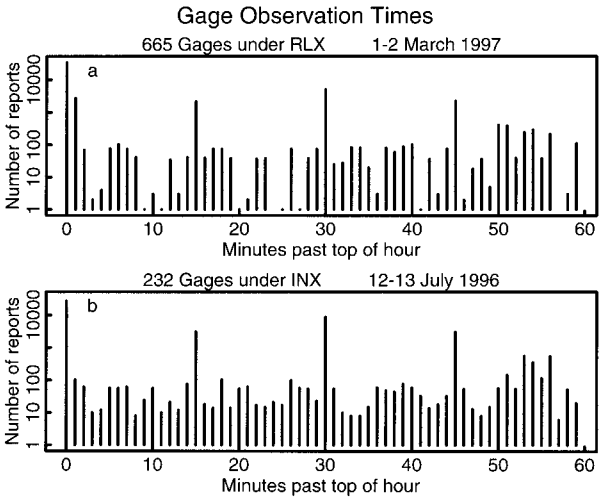

FIG. 6. Histogram of the number of gauge reports as a function of the observation time within the hour for the same gauge datasets as in Fig. 5 for the (a) RLX and (b) INX WSR-88Ds.

were chosen for analysis. These two radars are not necessarily representative of the situation at all other radars, particularly regarding the exceptionally large number of gauges available. They do, however, illustrate some of the differences in gauge network reporting characteristics across the country. Often there are delays of up to 4 h in receiving the full complement of gauge reports because DCPs are typically programmed to store 3 or 4 h of data before transmission to the GOES satellite. This time delay greatly reduces the amount of gauge data available to the PPS to perform real-time gauge–radar rainfall adjustments. Clearly the ability of the PPS to adjust radar rainfall estimates using real-time gauge data will be better at RLX than INX because of the more timely reporting characteristics of the gauges within the RLX domain. There is an initiative within the NWS to work with other federal agencies to reprogram their gauges to report more frequently for use by the PPS. Also, there are plans to enhance the adjustment algorithm to make use of late-reporting gauges.

Figure 6 is a histogram of times within the clock hour when rainfall measurements are collected by gauges for the same two radars and 48-h periods as in Fig. 5. The largest number of gauge measurements are collected at the top of the hour, with secondary maxima at H + 30, H + 15, and H + 45 min at both RLX and INX. The adaptable parameter representing the ending time of the hourly periods when the PPS performs gauge–radar adjustment (H + 00 minutes) is optimized using this information.

5. Current limitations and future challenges

Operational radar rainfall estimation presents unique challenges. The estimation algorithm must be rooted in scientific principles and be flexible enough to adapt to the latest scientific techniques. It must be robust enough to not only permit integration of technological advances over time but adapt in its current form to widely varying climatic, seasonal, synoptic, and mesoscale conditions. The algorithm must work in moist tropical climates in Hawaii, dry high plains climates in North Dakota, mountainous regions in Colorado, cool climates in Alaska, and everywhere else in between. In order to fully understand the rainfall products generated by the PPS, an understanding of their strengths and weaknesses is necessary. This section broadly reviews current deficiencies in the PPS and what the near future holds for operational radar rainfall processing in the NWS. Many of these operational deficiencies of the PPS are typical of radar rainfall algorithms used operationally in other parts of the world (WCRP 1996; Meischner et al. 1997). Although these problems have been known for decades, definitive, robust solutions (algorithmic or technological) are often either unavailable, not commonly agreed upon, and/or unaffordable.

a. Parameter optimization

The large number of adaptable parameters in the PPS is a sign that the original algorithm designers had enough insight to build flexibility into the algorithm. However, the mere existence of adaptable parameters is not the ultimate solution; those parameters must first be optimized as a function of climate, season, and rainfall system type in order to produce the optimum rainfall estimates from the existing algorithm. Because long records of WSR-88D rainfall data are just now becoming

available, the current PPS adaptable parameters can begin to be optimized through statistical studies.

The NWS and its collaborators are beginning to tackle the nonlinear, multidimensional optimization issue now that a few years of WSR-88D data have been archived (Anagnostou and Krajewski 1998). This parameter optimization effort is expected to continue for many years as longer records of radar rainfall over diverse climatic regions of the United States accumulate.

Of particular importance is the optimal estimation of *Z–R* parameters for various classifications of rainfall as well as the identification of environmental and/or storm-morphological parameters that physically relate to the cloud microphysical processes affecting the *Z–R* relationship. The current use of spatially uniform *Z–R* parameters will continue until a proven methodology for applying different *Z–R* parameters to different parts of a storm is developed. Automated and robust operational classification techniques valid over a wide range of rain systems in various seasons are needed to partition the rain systems into zones that have broadly similar microphysics and therefore similar *Z–R* parameters.

b. Bright band and snow

There are a number of major enhancements to current functionality that deserve attention. One is the issue of correcting for brightband enhancement and the more general problem of accounting for frozen or mixed-phase hydrometeors. The PPS, in its current form, is not capable of producing quantitatively reliable rainfall estimates where the radar beam is at or above the freezing level. The assumption of spherical liquid phase targets in the radar equation is violated. In addition, the *Z–R* equation assumes the existence of liquid hydrometeors, not frozen ones. As Joss and Waldvogel (1990) and others point out, much more research is needed in order to extract snowfall depth and/or liquid water equivalent of snow from radar measurements. The Bureau of Reclamation, in cooperation with the WSR-88D OSF, is developing an operational snow algorithm for the WSR-88D. Also, the NWS Hydrologic Research Laboratory continues to evaluate potential operational algorithms to mitigate brightband contamination or, more simply, to at least automatically locate the brightband altitude as qualitative information for the forecaster's use (Seo et al. 1997). A literature review reveals that there are no obvious or simple solutions to automated correction of the estimates, however.

c. Range degradation

One of the biggest problems with WSR-88D rainfall estimates has been range degradation (underestimation). The source of this problem is not primarily incomplete beam filling but the typical reduction of reflectivity with increasing altitude and the overshooting of the rain clouds (lack of detection) at far ranges, which requires a more complex solution. Smith et al. (1996a,b) show strong range degradation in WSR-88D rainfall estimates from about a dozen radars over a several-year period, which is partly attributable to the radar beam overshooting the rain at far ranges. The problem is greater in the cool seasons that are dominated by shallow, stratiform rainfall systems, as well as at mountainous sites where blockages obscure low tilt angles. Figure 3b illustrates this range effect for a cool season flooding event in Kentucky, Ohio, and Indiana, as evidenced by the large rainfall gradients at the farthest ranges.

If the radar is able to detect at least some small signal, it is possible to use a mean vertical reflectivity profile to extrapolate rainfall down to the ground [see, e.g., Joss and Waldvogel (1990) and Smith (1990) and references therein]. If the radar does not detect any signal from rainfall existing below the lowest beam, then the problem becomes more challenging. Existing and proposed real-time range correction algorithms that account for the vertical gradient of reflectivity are being examined for possible operational implementation within the PPS (Seo et al. 1996, 1997).

d. Reflectivity calibration and clutter suppression

Proper absolute calibration of the WSR-88D radar is a critical assumption of the PPS. Temporal and spatial integrity of WSR-88D calibration over the radar network remains a problem. Local automated self-calibration procedures have not proven to be robust and stable enough to maintain sufficient accuracy for satisfactory quantitative rainfall estimation at some sites. Also, occasional improper and excessive clutter suppression at some sites may cause real meteorological echoes to be unnecessarily removed and rainfall to be underestimated. Engineering work continues at the WSR-88D OSF to improve hardware calibration and clutter suppression techniques and to enhance the training of radar operators and forecasters. It is hoped that the deployment of the GDS capability and resulting gauge–radar bias adjustments will help to correct for reflectivity calibration biases. Gauge–radar bias statistics are currently being compiled and monitored by HRL to quantify the impact of this problem.

e. Anomalous propagation

Improved and robust automated quality control techniques that make use of Doppler radial velocity and spectrum-width data beyond what is done with the existing signal processing techniques within the RDA are needed to remove transient areas of anomalous propagation, particularly when that contamination coexists simultaneously with real-rain echoes. Capabilities currently exist within the WSR-88D system to manually define transient clutter suppression regions (see section 2), however, that capability depends on the ability of the radar operators to recognize it and react quickly.

The existing PPS tilt test algorithm is most effective when anomalous propagation echoes occur in the absence of rain echoes. Improved quality control techniques are being investigated in cooperation with NWS collaborators (Smith et al. 1996b, 1997).

f. Local gauge–radar bias correction

Local gauge–radar biases arise from a number of sources. These include spatially variable rainfall microphysics within the cloud system combined with the forced use of spatially uniform, and perhaps inappropriate, *Z–R* parameters in the PPS. There may also be range-dependent biases from radar beam overshooting of the rain cloud (see section 5c) as well as azimuth-dependent biases, or ''shadows,'' resulting from beam blockages by surrounding terrain. Dense gauge networks allow us the opportunity to correct these error sources. Though currently limited in number, there exist gauge-rich WSR-88D sites where real-time local bias corrections are possible. Although an algorithm incorporating this capability exists in follow-on processing in stage II (section 6a), implementation of such an algorithm within the PPS deserves consideration.

g. Attenuation

Ryzhkov and Zrnić (1995) show results from an intense squall line case in Oklahoma indicating that attenuation may have a greater impact on S-band WSR-88D rainfall estimates than previously thought. There is currently no accounting in either the PPS algorithm or the RDA for attenuation by intervening rain or a wet radome.

h. Dual polarization

The WSR-88D is a horizontal linear polarization radar. Dual polarization radar measurements of specific differential phase at two orthogonal polarizations (horizontal and vertical) have shown skill in improving rainfall estimates compared to single polarization radars using *Z–R* relationships (Ryzhkov and Zrnić 1996a,b). Also, additional hydrometeor microphysical information can be inferred with the addition of vertical polarization measurements to obtain differential reflectivity as an aid in hydrometeor size and type identification (rain, hail, snow) and improved rainfall estimation (Seliga and Bringi 1976; Illingworth and Caylor 1989).

The NWS is investigating the possibility of implementing polarimetric technology in the future on the WSR-88Ds in order to improve rainfall estimation and for other nowcasting applications. The NOAA National Severe Storms Laboratory is leading an effort to retrofit an existing WSR-88D in Oklahoma as a prototype testbed for operational demonstration. Zrnić (1996) suggests that polarimetric technology shows great promise for operational applications in hydrology. There is, however, a need to first prove that the operational benefits exceed the costs before full-scale deployment will be considered.

6. Overview of follow-on rainfall processing

The precipitation processing system has been designed as an integrated, end-to-end forecast system that culminates in the passing of hourly radar and gauge rainfall data into the NWS River Forecast System (NWSRFS) to support the river forecasting mission of the NWS (Fread et al. 1995; Hudlow 1988). The NWSRFS is a set of RFC hydrologic models that have been calibrated using historical gauge data. Efforts are under way to incorporate gridded hourly radar rainfall data into the models on a nationwide basis. The PPS running on the WSR-88D RPG is the first processing step (''stage I'') in this integrated processing stream. There are two additional stages of rainfall processing performed at the RFCs to add value to the radar estimates from stage I and to improve hydrologic forecasting (Hudlow et al. 1983, 1991). This section provides a brief overview of this subsequent processing external to the WSR-88D.

a. Stage II

The main purpose of stage II is to provide an optimal estimate of hourly rainfall using a multivariate objective analysis scheme incorporating both radar and raingauge observations. This multisensor estimate of rainfall is performed once per hour on UNIX workstations for each radar on the HRAP grid using as input the hourly digital precipitation array product from stage I (Fig. 7a) and all available rain gauge data (objectively analyzed in Fig. 7b). The first step in creating this radar–gauge multisensor estimate is to compute and apply a new mean field gauge–radar bias using a statistical Kalman filter approach similar to that used in stage I (Fig. 7c). Because the gauge data communication system for the stage II algorithm is different and less complicated than that for the PPS algorithm on the WSR-88D RPG, and because it has been in place since the early 1990s at several RFCs, hourly gauge–radar biases have been computed operationally in stage II (unlike in stage I) and have been adjusting WSR-88D rainfall products used by several of the river forecast centers for at least five years now. Nearly all RFCs are now currently executing stage II.

Biases in radar-derived rainfall may vary nonuniformly over the radar domain as a function of range, azimuth, rainfall type, and other factors. To account for this spatial inhomogeneity, the second processing step in stage II (after the mean field bias correction) is the local adjustment to the rainfall estimates using a multivariate optimal estimation procedure that incorporates point gauge data into the rainfall analysis-

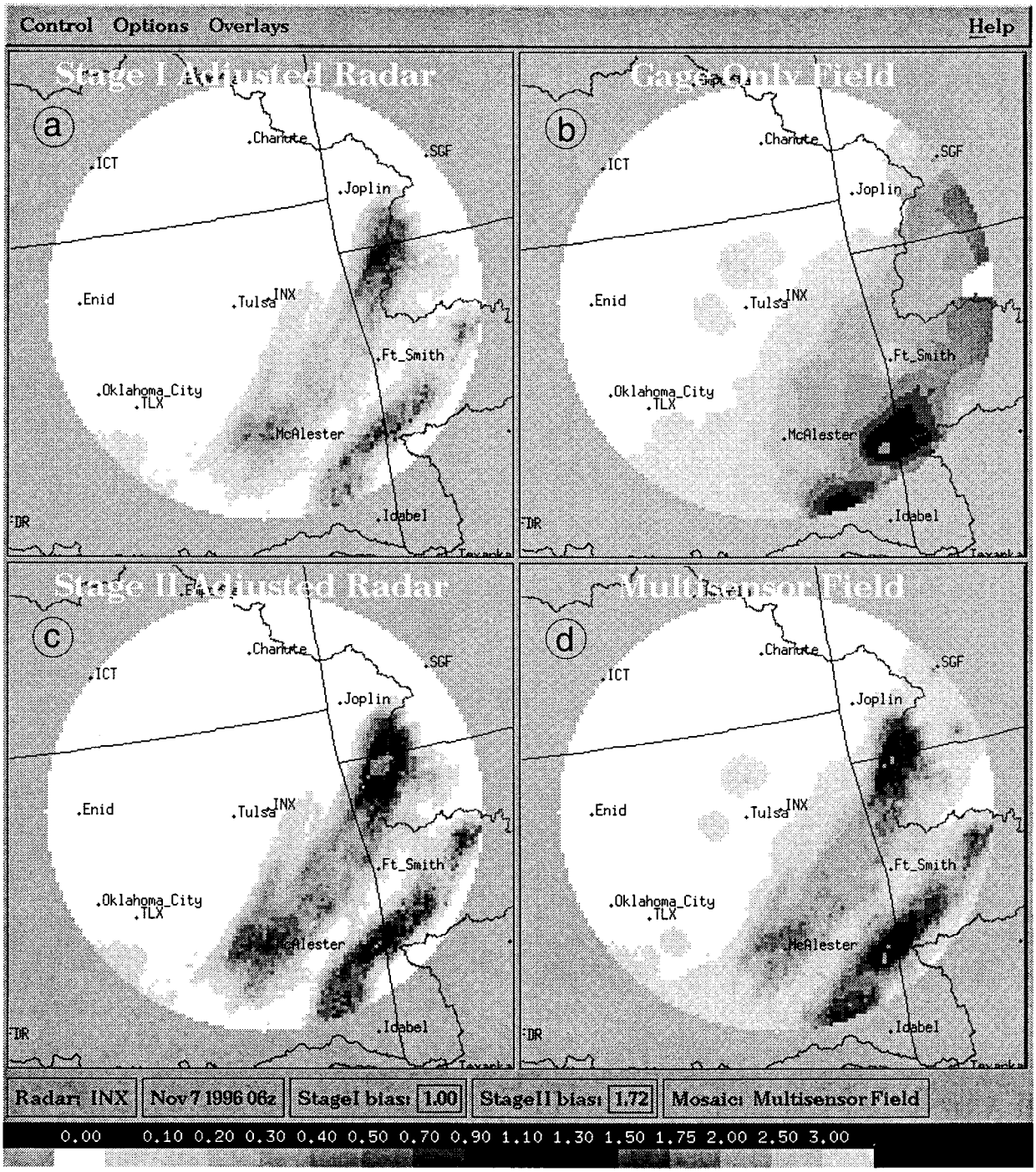

FIG. 7. One-hour rainfall accumulation (in.) ending at 0600 UTC 7 November 1996 for the INX WSR-88D estimated from (a) stage I bias-adjusted radar only (i.e., the DPA product), (b) rain gauges only, (c) stage II bias-adjusted radar only, and (d) stage II radar-rain gauge multisensor optimal estimate.

(Seo 1998). The rainfall field that results is called the ''multisensor'' analysis (Fig. 7d). In this objective analysis procedure, the weights for radar and gauge estimates at each HRAP grid point are determined such that their linear combination minimizes the expected error variance of the estimate. A decreasing (increasing) weight is placed on the gauge (radar) accumulation as the distance increases away from the gauge. In the future, real-time satellite rainfall estimates from infrared and/or passive microwave techniques may eventually be incorporated into the optimal analysis algorithm as a third independent measure of rainfall, par-

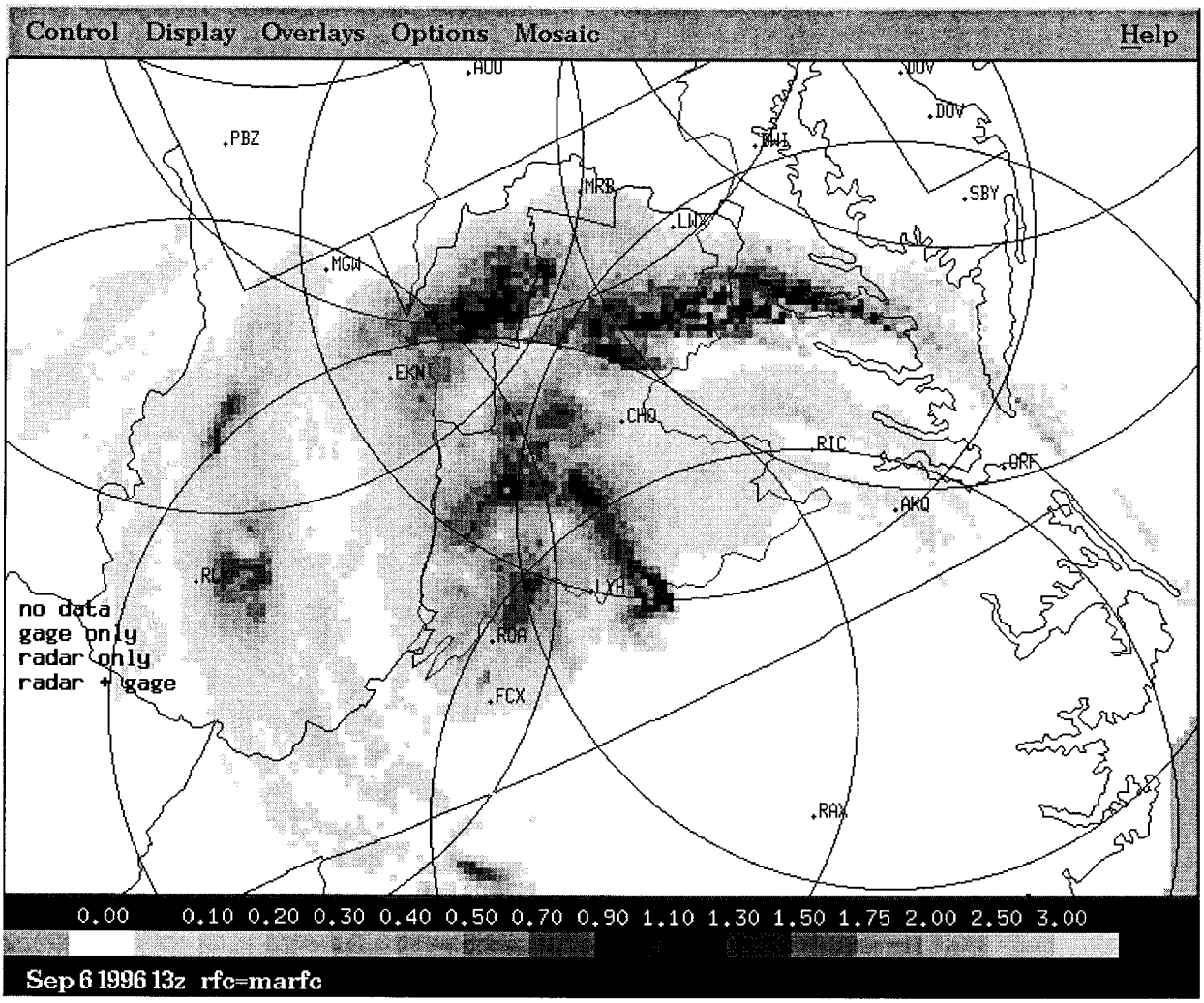

FIG. 8. Stage III 1-h rainfall accumulation (in.) ending at 1300 UTC 6 September 1996 covering the Middle Atlantic RFC area. This composite, associated with the remnants of Hurricane Fran centered in southwest Virginia, was constructed by mosaicking stage II multisensor estimates from 12 overlapping radars. The rings represent the 230-km range limit of stage II processing for each of these radars.

ticularly in those areas where the radar is blocked by mountains or where there are no gauges.

Because the stage II algorithm does not have the gauge timeliness restriction (50 min) and gauge network restriction (50 gauges) imposed in stage I, it should produce more representative bias estimates because more gauge data will be available. However, the relaxation of these gauge number and timeliness requirements comes at the expense of less timely rainfall estimates. This handicap is not so severe for the RFCs because they are primarily responsible for forecasting longer timescale flooding events. On the other hand, the weather forecast offices (WFOs) are primarily responsible for short timescale flash flood forecasting and warning, and therefore the stage II estimates may not necessarily provide WFOs significant additional value above and beyond that provided by the stage I gauge-adjusted rainfall products.

b. Stage III

RFCs need regional rainfall estimates over a much larger area than that covered by an individual radar. Stage III is the third stage of NWS rainfall processing, and it is designed to mosaic stage II multisensor estimates from multiple radars on the national HRAP grid covering the RFC's forecast area. An example of a stage III hourly rainfall estimate from the Middle Atlantic RFC is shown in Fig. 8.

Stage III provides a graphical user interface to display the composited rainfall estimates and to allow interactive quality control of both gauge and radar data for each radar (Shedd and Smith 1991; Shedd and Fulton 1993). It represents the only step in the three rainfall processing stages that allows human intervention before the data are finally sent to the hydrologic models. The gauge and radar estimates can be manually edited to

remove bad data or areas contaminated by anomalous propagation or other sources of error.

The NWSRFS models currently operate on a 6-h time step and aggregate input gauge and radar rainfall data in terms of basin averages. To obtain the mean areal precipitation from stage III estimates for each basin for input into the models, the hourly stage III gridded estimates are averaged spatially and then summed over a 6-h period. Work is under way among the Hydrologic Research Laboratory, its collaborators, and other groups to improve the operational hydrologic modeling techniques so that the high spatial and temporal resolution radar estimates are fully utilized (Finnerty et al. 1997).

c. Stage IV

The NWS's National Centers for Environmental Prediction are leading an effort to assimilate gridded WSR-88D-derived precipitation estimates into their atmospheric forecast models to improve precipitation forecasts (Lin et al. 1997). To accomplish this goal, stage II rainfall products for all radars are being generated and composited on the national HRAP grid to produce a stage IV rainfall estimate over the entire United States (Baldwin and Mitchell 1997). These estimates do not currently incorporate the mean field bias adjustment nor manual quality control procedures performed by the RFCs; however, there are plans to incorporate the adjusted and manually edited stage III products from the RFCs when and where they are available.

7. Concluding remarks

This paper describes the WSR-88D rainfall algorithm and its current strengths and limitations. It also outlines several areas that represent opportunities for research. WSR-88D rainfall estimates over the entire United States are now a reality. Not only is the forecasting and warning mission of the NWS benefitting but so is a wide variety of natural disaster mitigation and water resources management activities among a variety of government and commercial organizations. The algorithm is expected to evolve and improve over time as the WSR-88D transitions to an open-standard hardware platform in the coming years and as experience grows.

Acknowledgments. The authors sincerely appreciate the reviews provided by NWS forecasters Paul Jendrowski, Robert Shedd, Mark Walton, and the anonymous reviewers as well as valuable discussions and collaboration with Profs. Witold Krajewski and James Smith.

REFERENCES

Ahnert, P., M. Hudlow, E. Johnson, D. Greene, and M. Rosa Dias, 1983: Proposed ''on-site'' precipitation processing system for NEXRAD. Preprints, *21st Conf. on Radar Meteorology,* Edmonton, AB, Canada, Amer. Meteor. Soc., 378–385.

——, ——, and ——, 1984: Validation of the ''on-site'' precipitation processing system for NEXRAD. Preprints, *22d Conf. on Radar Meteor.,* Zurich, Switzerland, Amer. Meteor. Soc., 192–201.

——, W. Krajewski, and E. Johnson, 1986: Kalman filter estimation of radar-rainfall field bias. Preprints, *23*rd *Conf. on Radar Meteor.,* Snowmass, CO, Amer. Meteor. Soc., JP33–JP37.

Anagnostou, E., and W. Krajewski, 1998: Calibration of the WSR-88D Precipitation Processing Subsystem. *Wea. Forecasting,* **13,** 396–406.

Austin, P., 1987: Relation between measured radar reflectivity and surface rainfall. *Mon. Wea. Rev.,* **115,** 1053–1070.

Baldwin, M., and K. Mitchell, 1997: The NCEP hourly multi-sensor U.S. precipitation analysis for operations and GCIP research. Preprints, *13th Conf. on Hydrology,* Long Beach, CA, Amer. Meteor. Soc., 54–55.

Battan, L., 1973: *Radar Observation of the Atmosphere.* University of Chicago Press, 324 pp.

Chrisman, J., D. Rinderknecht, and R. Hamilton, 1994: WSR-88D clutter suppression and its impact on meteorological data interpretation. Preprints, *First WSR-88D User's Conference,* Norman, OK, WSR-88D Operational Support Facility, 9–20.

Crum, T., and R. Alberty, 1993: The WSR-88D and the WSR-88D Operational Support Facility. *Bull. Amer. Meteor. Soc.,* **74,** 1669–1687.

Doviak, R., 1983: A survey of radar rain measurement techniques. *J. Climate Appl. Meteor.,* **22,** 832–849.

——, and D. Zrnić, 1984: *Doppler Radar and Weather Observations.* Academic Press, 458 pp.

Finnerty, B., M. Smith, D.-J. Seo, V. Koren, and G. Moglen, 1997: Space–time scale sensitivity of the Sacramento model to radar–gauge precipitation inputs. *J. Hydrol.,* **203,** 21–38.

Fread, D., and Coauthors, 1995: Modernization in the National Weather Service river and flood program. *Wea. Forecasting,* **10,** 477–484.

Gelb, A., Ed., 1974: *Applied Optimal Estimation.* The MIT Press, 374 pp.

Heiss, W., D. McGrew, and D. Sirmans, 1990: NEXRAD: Next Generation Weather Radar (WSR-88D). *Microwave J.,* **33,** 79–98.

Hudlow, M., 1988: Technological developments in real-time operational hydrologic forecasting in the United States. *J. Hydrol.,* **102,** 69–92.

——, D. Greene, P. Ahnert, W. Krajewski, T. Sivaramakrishnan, and E. Johnson, 1983: Proposed off-site precipitation processing system for NEXRAD. Preprints, *21st Conf. on Radar Meteor.,* Edmonton, AB, Canada, Amer. Meteor. Soc., 394–403.

——, J. Smith, M. Walton, and R. Shedd, 1991: NEXRAD: New era in hydrometeorology in the USA. *Hydrological Applications of Weather Radar,* I. Cluckie and C. Collier, Eds., Ellis Horwood Limited, 602–612.

Hunter, S., 1996: WSR-88D radar rainfall estimation: Capabilities, limitations and potential improvements. *NWA Digest,* **20** (4), 26–36.

Illingworth, A., and I. Caylor, 1989: Polarization radar estimates of raindrop size spectra and rainfall rates. *J. Atmos. Oceanic Technol.,* **6,** 939–949.

Joss, J., and A. Waldvogel, 1990: Precipitation measurement and hydrology. *Radar in Meteorology,* D. Atlas, Ed., Amer. Meteor. Soc., 577–606.

Kelsch, M., 1992: Estimating maximum convective rainfall rates for radar-derived accumulations. Preprints, *Fourth AES/CMOS Workshop on Operational Meteor.,* Whistler, BC, Canada, Amer. Meteor. Soc., 161–168.

Klazura, G., and D. Imy, 1993: A description of the initial set of analysis products available from the NEXRAD WSR-88D system. *Bull. Amer. Meteor. Soc.,* **74,** 1293–1311.

——, and S. Kelly, 1995: A comparison of high resolution precipitation algorithm with rain gauge data. Preprints, *27th Conf. on Radar Meteor.,* Vail, CO, Amer. Meteor. Soc., 31–34.

Larson, L., and Coauthors, 1995: Operational responsibilities of the

National Weather Service river and flood program. *Wea. Forecasting,* **10,** 465–476.

Lin, Y., K. Mitchell, E. Rogers, and M. Baldwin, 1997: Assimilation of hourly precipitation data to improve the water cycle components of NCEP's Eta Model. Preprints, *13th Conf. on Hydrology,* Long Beach, CA, Amer. Meteor. Soc., 52–53.

Meischner, P., C. Collier, A. Illingworth, J. Joss, and W. Randeu, 1997: Advanced weather radar systems in Europe: The COST 75 Action. *Bull. Amer. Meteor. Soc.,* **78,** 1411–1430.

O'Bannon, T., 1997: Using a 'terrain-based' hybrid scan to improve WSR-88D precipitation estimates. Preprints, *28th Conf. on Radar Meteorology,* Austin, TX, Amer. Meteor. Soc., 506–507.

OFC, 1991: Doppler radar meteorological observations, Part C, WSR-88D products and algorithms. Federal Meteorological Handbook 11, FCM-H11C-1991, Office of the Federal Coordinator for Meteorological Services and Supporting Research, Silver Spring, MD, 210 pp.

——, 1992: Doppler radar meteorological observations, Part D, WSR-88D unit description and operational applications. Federal Meteorological Handbook 11, FCM-H11D-1992, Office of the Federal Coordinator for Meteorological Services and Supporting Research, Silver Spring, MD, 208 pp.

Rosenfeld, D., D. Wolff, and D. Atlas, 1993: General probability-matched relations between radar reflectivity and rain rate. *J. Appl. Meteor.,* **32,** 50–72.

Ryzhkov, A., and D. Zrnić, 1995: Precipitation and attenuation measurements at a 10-cm wavelength. *J. Appl. Meteor.,* **34,** 2121–2134.

——, and ——, 1996a: Rain in shallow and deep convection measured with a polarimetric radar. *J. Atmos. Sci.,* **53,** 2990–2995.

——, and ——, 1996b: Assessment of rainfall measurement that uses specific differential phase. *J. Appl. Meteor.,* **35,** 2080–2090.

Sauvageot, H., 1994: Rainfall measurement by radar: A review. *Atmos. Res.,* **35,** 27–54.

Schaake, J., 1989: Importance of the HRAP grid for operational hydrology. Preprints, *U.S./People's Republic of China Flood Forecasting Symp.,* Portland, OR, NOAA/NWS, 331–355.

Seliga, T., and V. Bringi, 1976: Potential use of radar differential reflectivity measurements at orthogonal polarizations for measuring precipitation. *J. Appl. Meteor.,* **15,** 69–76.

Seo, D.-J., 1998: Optimal estimation of rainfall fields using radar rainfall and rain gauge data. *J. Hydrol.,* in press.

——, R. Fulton, J. Breidenbach, D. Miller, and E. Friend, 1995: Final report. Interagency Memorandum of Understanding among the NEXRAD Program, WSR-88D Operational Support Facility, and the NWS/OH Hydrologic Research Laboratory, 51 pp. [Available from NWS/OH/HRL, 1325 East–West Hwy., W/OH1, Silver Spring, MD 20910.]

——, ——, ——, M. Taylor, and D. Miller, 1996: Final report. Interagency Memorandum of Understanding among the NEXRAD Program, WSR-88D Operational Support Facility, and the NWS/OH Hydrologic Research Laboratory, 64 pp. [Available from NWS/OH/HRL, 1325 East–West Hwy., W/OH1, Silver Spring, MD 20910.]

——, ——, and ——, 1997: Final report. Interagency Memorandum of Understanding among the NEXRAD Program, WSR-88D Operational Support Facility, and the NWS/OH Hydrologic Research Laboratory, 121 pp. [Available from NWS/OH/HRL, 1325 East–West Hwy., W/OH1, Silver Spring, MD 20910.]

Shedd, R., and J. Smith, 1991: Interactive precipitation processing for the modernized National Weather Service. Preprints, *Seventh Int. Conf. on Interactive Info. and Processing Systems for Meteorology, Hydrology, and Oceanography,* New Orleans, LA, Amer. Meteor. Soc., 320–323.

——, and R. Fulton, 1993: WSR-88D precipitation processing and its use in National Weather Service hydrologic forecasting. *Proc. Int. Symp. on Engineering Hydrology,* San Francisco, CA, ASCE, 16–21.

——, ——, and M. Walton, 1991: Sectorized hybrid scan strategy of the NEXRAD precipitation-processing system. *Hydrological Applications of Weather Radar,* I. Cluckie and C. Collier, Eds., Ellis Horwood Limited, 151–159.

Smith, J. A., and W. Krajewski, 1991: Estimation of the mean field bias of radar rainfall estimates. *J. Appl. Meteor.,* **30,** 397–412.

——, D.-J. Seo, M. Baeck, and M. Hudlow, 1996a: An intercomparison study of NEXRAD precipitation estimates. *Water Resour. Res.,* **32,** 2035–2045.

——, M. Baeck, M. Steiner, B. Bauer-Messmer, W. Zhao, and A. Tapia, 1996b: Hydrometeorological assessments of the NEXRAD rainfall algorithms. Final Rep. between Princeton University and the NWS/OH/Hydrologic Research Laboratory, 55 pp. [Available from NWS/OH/HRL, 1325 East–West Hwy., W/OH1, Silver Spring, MD 20910.]

——, ——, ——, and A. Miller, 1996c: Catastrophic rainfall from an upslope thunderstorm in the central Appalachians: The Rapidan storm of June 27, 1995. *Water Resour. Res.,* **32,** 3099–3113.

——, ——, and ——, 1997: Hydrometeorological assessments of the NEXRAD rainfall algorithms. Final Rep. between Princeton University and the NWS/OH/Hydrologic Research Laboratory, 59 pp. [Available from NWS/OH/HRL, 1325 East–West Hwy., W/OH1, Silver Spring, MD 20910.]

Smith, P, 1990: Precipitation measurement and hydrology: Panel report. *Radar in Meteorology,* D. Atlas, Ed., Amer. Meteor. Soc., 607–618.

Stallings, E., and L. Wenzel, 1995: Organization of the river and flood program in the National Weather Service. *Wea. Forecasting,* **10,** 457–464.

Wilson, J., and E. Brandes, 1979: Radar measurement of rainfall—A summary. *Bull. Amer. Meteor. Soc.,* **60,** 1048–1058.

World Climate Research Programme, 1996: BALTEX radar research—A plan for future action. Int. BALTEX Secretariat Publ. 6, Geesthacht, Germany, 46 pp.

Zrnić, D., 1996: Weather radar polarimetry—Trends toward operational applications. *Bull. Amer. Meteor. Soc.,* **77,** 1529–1534.